M-dwarfs and Stellar Standards with the FunnelWeb Star Survey

Adam D. Rains

PhD Thesis Proposal
The Australian National University

June 2017

Executive Summary

The FunnelWeb Star Survey, beginning in September 2017, will be the Southern Hemisphere's largest spectroscopic survey for years to come, targeting all stars, bar those in the most crowded regions of the Galaxy, brighter than Gaia G=12, along with selected supplementary surveys, with key science drivers of spectra for TESS planet hosts, Galactic archaeology, and young stars. To facilitate such science, FunnelWeb will employ a data-driven classification pipeline approach, using a comprehensive set of stellar spectral standards spanning the multi-dimensional stellar parameter space (e.g. spectral type, T_{Eff}, log(g), metallicity, and abundances). In doing so, FunnelWeb will characterise the Southern Hemisphere's M-dwarf population, with important implications for both stellar and exoplanetary science. Commencing 30/01/2017 and finishing no later than 30/07/2020, this PhD will be closely linked with the FunnelWeb Star Survey and aims to:

1. Constrain the T_{Eff} scale of dwarf and sub-giant stellar spectral standards in the Southern Hemisphere with precision interferometry,
2. Develop a data driven pipeline for FunnelWeb stellar classification, trained upon a comprehensive set of stellar standards, and capable of classifying M-dwarfs,
3. Produce a catalogue of Southern Hemisphere M-dwarfs, complete with fundamental stellar parameters, as observed by FunnelWeb,
4. Conduct an exploration into constraining the T_{Eff} scale of M-dwarfs specifically through the locating and characterisation of Southern Hemisphere M-dwarf double-lined eclipsing binaries, enabled by transiting exoplanet surveys.

Chapter 1

Background

1.1 Motivation

The FunnelWeb Star Survey, beginning in September 2017 and enabled by the TAIPAN instrument on the UK-Schmidt Telescope, will be the Southern Hemisphere's largest spectroscopic survey for years to come. Targeting all stars, bar those in the most crowded regions of the Galaxy, brighter than Gaia G=12 magnitude, along with selected supplementary surveys, the survey has key science drivers of spectra for TESS planet hosts, Galactic archaeology, and young stars. To facilitate such science, FunnelWeb will employ a data-driven classification pipeline approach, deriving accuracy not from theoretical models and spectral line lists, but from a comprehensive set of stellar spectral standards spanning the multi-dimensional stellar parameter space. Such standards will have precise observationally derived fundamental stellar parameters (e.g. spectral type, T_{Eff}, log(g), metallicity, and abundances), taken from past literature, or observed by FunnelWeb personnel for particularly sparse regions of the parameter-space.

FunnelWeb thus aims to deliver T_{Eff} for every star observed, but this places strict requirements on the accuracy of its selected standards. It is not yet possible to calibrate the T_{Eff} scale at $< 100\,K$ from spectra alone, as non-LTE and 3D effects of the associated models and line lists become important, particularly where log(g) and [Fe/H] remain uncertain (e.g. Yong et al. 2004; Bensby et al. 2014)). Angular diameters however provide a direct approach to T_{Eff} determination when combined with bolometric flux measurements, with the highest precision measurements being at the $\sim 1\,\%$ level. Such measurements will thus act as crucial standards for FunnelWeb. Additionally, the low-mass end of the HR-diagram, particularly M-dwarfs, pose a problem for model based classification, with stellar radii historically not well reproduced by evolutionary models (e.g. Ribas et al. 2008). Given reliable stellar standards, it is expected a data driven approach will prove advantageous.

M-dwarfs are of increasing importance to exoplanet research, particularly in the hunt for Earth-like planets in the stellar habitable zone. Their low masses and luminosities mean that photometric (i.e. exoplanet stellar transits) and spectroscopic (i.e radial velocity) searches are more sensitive to smaller, low-mass planets, with the recent discovery of seven terrestrial planets orbiting TRAPPIST-1 (Gillon et al. 2017), a cool ($T_{Eff} \approx 2559\,K$) M-dwarf, a particularly noteworthy example. Exoplanet research benefits from well-constrained stellar parameters, both to better characterise those planets already detected, but also to inform targeted surveys (e.g. the Transiting Exoplanet Survey Satellite, or TESS, mission) of stars likely to host planets. There exists a well-known planet-metallicity correlation for hot Jupiters (e.g. Gonzalez 1997; Fischer & Valenti 2005; Sousa et al. 2008; Neves et al. 2013; Wang & Fischer 2015; Buchhave & Latham

2015), but to to extend this to an M-dwarf context requires robust abundance determination, a process hampered by degeneracies between metallicity and mass/T_{Eff} (e.g. Neves et al. 2012). Additional concerns arise when stars initially classified as dwarfs are found to be giants upon further analysis (Mann et al. 2012), boding poorly for planet detection. Thus there is a need for precise, *reliable* stellar parameters to enable stellar and exoplanetary research.

1.1.1 Project Overview and Outline

Working with the FunnelWeb Star Survey, this PhD aims to:

1. Constrain the T_{Eff} scale of dwarf and sub-giant stellar spectral standards in the Southern Hemisphere with precision interferometry,
2. Develop a data driven pipeline for FunnelWeb stellar classification, trained upon a comprehensive set of stellar standards, and capable of classifying M-dwarfs,
3. Produce a catalogue of Southern Hemisphere M-dwarfs, complete with fundamental stellar parameters, as observed by FunnelWeb,
4. Conduct an exploration into constraining the T_{Eff} scale of M-dwarfs specifically through the locating and characterisation of Southern Hemisphere M-dwarf. double-lined eclipsing binaries, enabled by transiting exoplanet surveys

The remainder of Chapter 1 summarises necessary background, with Chapter 2 going into greater detail on the PhD research, resources, and timeline.

1.2 Fundamental Stellar Parameters

1.2.1 Flux

The monochromatic flux of a star is the power per unit area per wavelength ($\mathrm{W\,m^{-2}\,m^{-1}}$). The bolometric flux instead is a measure of the flux integrated over *all* wavelengths, and is thus not the result of a single observation. It can be defined as follows:

$$F_* = \int_0^\infty F_\lambda d\lambda \tag{1.1}$$

where:

- F_λ is the stellar flux in $\mathrm{W\,m^{-2}\,m^{-1}}$,
- F_* is the bolometric stellar flux, the flux over all wavelengths, in $\mathrm{W\,m^{-2}}$.

In terms of *observable* quantities, the flux received at Earth is given by the ratio between the spheres defining the surface of the star and Earth:

$$\begin{aligned} f_E &= \frac{4\pi R^2}{4\pi D^2} F_* \\ &= \left(\frac{R}{D}\right)^2 F_* \end{aligned}$$

where D is the distance to the star.

Trigonometry and the small angle approximation can be used to relate D and R to the on-sky angle:

$$\tan\frac{\theta}{2} = \frac{R}{D} \tag{1.2}$$

$$\theta \approx \frac{2R}{D} \tag{1.3}$$

Thus, the bolometric flux, put in terms of the flux received at Earth can be written in the following ways:

$$F_* = \frac{4}{\theta^2} f_E \tag{1.4}$$

$$F_* = \left(\frac{D}{R}\right)^2 f_E \tag{1.5}$$

1.2.2 Magnitude

The bolometric magnitude of a star is given by the following relation, as per the Mamajek et al. (2015) IAU resolution:

$$M_{\text{bol}} = -2.5 \log_{10} L + 71.197425 \tag{1.6}$$

where:

- M_{bol} is the bolometric magnitude of the star,
- L is the luminosity of the star in W,
- 71.197425 is a zero point defined using the *nominal solar luminosity* ($L_\odot^N = 3.828 \times 10^{26}\,\text{W}$), corresponding to $M_{\text{bol}\odot} \approx 4.74\,\text{mag}$.

1.2.3 Luminosity

Stellar luminosity and flux can be related as follows:

$$L = F_* A \tag{1.7}$$

where A is the surface area of the star. Taking A to be spherical and defined by a radius R, the flux-luminosity relation becomes:

$$L = 4\pi R^2 F_* \tag{1.8}$$

1.2.4 Effective Temperature

Stellar temperatures are an important property of stars, but are difficult to measure accurately from Earth (and ultimately vary depending on the depth considered). A useful approach is thus to approximate a star as a black body with the same luminosity per surface area as the star itself (at a given depth, such as the stellar "surface"). This relates luminosity, temperature, and surface area as follows using the Stefan-Boltzmann equation for a black body:

$$L = \sigma A T^4 \tag{1.9}$$

where:

- L is the luminosity in W,
- σ is the Stefan-Boltzmann constant in $\mathrm{W\,m^{-2}\,K^{-4}}$,
- A is the illuminated surface area in $\mathrm{m^2}$,
- T is the temperature of the body in K.

Such an approximation is exactly that, so the temperature calculated from this relation is referred to as the *effective temperature* - T_{Eff}. Taking the spherical flux-luminosity relationship from Equation 1.8, the luminosity of a star can be shown to depend on both its temperature and radius:

$$L = 4\pi R^2 \sigma {T_{\mathrm{Eff}}}^4 \tag{1.10}$$

Written another way, $\mathrm{T_{Eff}}$ can be put in terms of an *angular* stellar diameter (as obtained via interferometry):

$$F_\lambda = \frac{4}{{\theta_{\mathrm{LD}}}^2} f_\lambda$$
$$\sigma {T_{\mathrm{Eff}}}^4 = \frac{4}{{\theta_{\mathrm{LD}}}^2} \int_0^\infty f_\lambda d\lambda$$

where:

- F_λ, as before, is the stellar *surface* flux in $\mathrm{W\,m^{-2}\,m^{-1}}$,
- f_λ is the *received* stellar flux (corrected for interstellar extinction) in $\mathrm{W\,m^{-2}\,m^{-1}}$
- θ_{LD} is the *limb-darkened* stellar angular diameter in radians.

Thus $\mathrm{T_{Eff}}$ can be obtained observationally through combination of θ_{LD} and f_{bol} (the *received* bolometric flux), or the combination of L (stellar luminosity, requiring a distance/parallax measurement) and R (the stellar radius).

1.2.5 Surface Gravity

The surface gravity of a spherical astronomical body (i.e. a star) can be calculated from Newton's law of universal gravitation:

$$g = \frac{GM}{R^2} \tag{1.11}$$

where:

- g is the surface gravity in $\mathrm{m\,s^{-2}}$,
- G is the gravitational constant in $\mathrm{m^3\,kg^{-1}\,s^{-2}}$,
- M is the mass of the body in kg,
- R is the radius of the body in m.

1.2.6 Colour

The magnitudes of stars measured in different filter passbands can be compared to gain insight into the slope of the stellar spectrum and thus aid in classification. Figure 1.1 illustrates the standard U (ultraviolet), B (blue), V (visible) photometric system, whereas Figure 1.2 demonstrates the relationship between spectral type and B-V colour index.

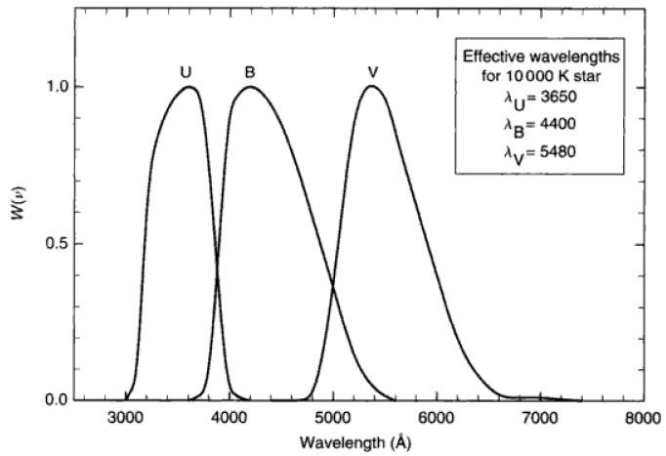

Figure 1.1: Response functions for the standard Johnson photometric system (Johnson 1965; Gray 2008)

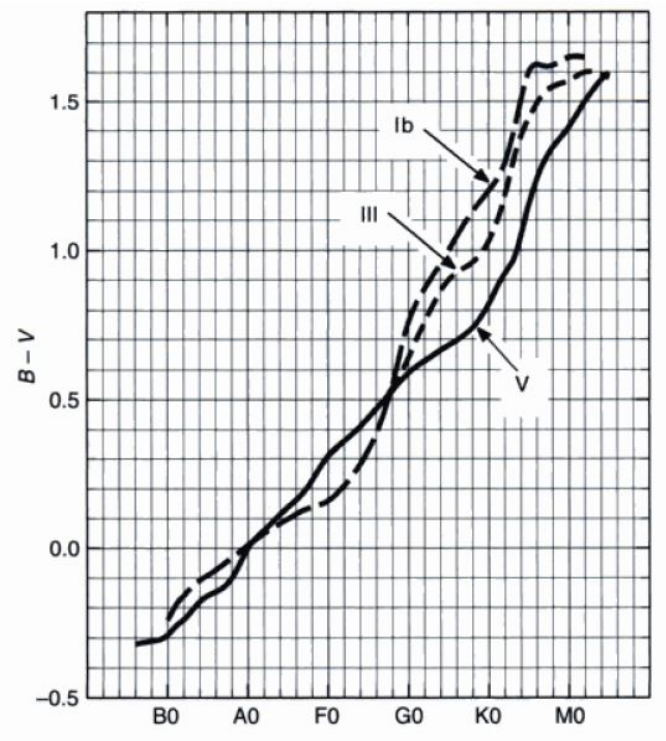

Figure 1.2: Relationship between B-V colour index and spectral type (Fitzgerald 1970; Gray 2008)

1.3 Stellar Classification

Stars can be placed in both a *spectral* class and a *luminosity* class, forming the basis of the historic Morgan-Keenan (MK) classification system.

1.3.1 Spectral Classification

The spectral type of a star comes from the Harvard system, broken up using the labels OBAFGKM (as per Table 2.2) followed by an Arabic numeral in the range 0-9 to further subdivide (with 0 being the hottest star in each class). The system essentially tracks the effective temperature of the star.

Table 1.1: Spectral classification (Habets & Heintze 1981)

Class	T_{EFF}	**Main Sequence**		
		Mass	**Radius**	**Luminosity**
O	≥30,000 K	≥16 $M_\odot$	≥6.6 $R_\odot$	≥30,000 $L_\odot$
B	10,000-30,000 K	2.1-16 $M_\odot$	1.8-6.6 $R_\odot$	25-30,000 $L_\odot$
A	7,500-10,000 K	1.4-2.1 $M_\odot$	1.4-1.8 $R_\odot$	5-25 $L_\odot$
F	6,000-7,500 K	1.04-1.4 $M_\odot$	1.15-1.4 $R_\odot$	1.5-5 $L_\odot$
G	5,200-6,000 K	0.8-1.04 $M_\odot$	0.96-1.15 $R_\odot$	0.6-1.5 $L_\odot$
K	3,700-5,200 K	0.45-0.8 $M_\odot$	0.7-0.96 $R_\odot$	0.08-0.6 $L_\odot$
M	2,400-3,700 K	0.08-0.45 $M_\odot$	≤0.7 $R_\odot$	≤0.08 $L_\odot$

1.3.2 Luminosity Classification

Luminosity and pressure (at unity optical depth) of a star are strongly correlated, enabling for the historical classes shown in Table 1.2. Such a correlation stems from the fact that stars with a higher surface gravity (i.e. a high density) show greater pressure broadening of spectral lines. This serves as a way to differentiate stars of varying surface gravity (e.g. a giant vs a dwarf).

Table 1.2: Luminosity classification (Gray 2008)

Class	**Star**
O	Hypergiants
Ia	Luminous supergiants
Ib	Less luminous supergiants
II	Bright giants
III	Normal giants
IV	Subgiants
V	Main sequence dwarfs
VI or sd	Subdwarfs

1.3.3 The Hertzsprung-Russell Diagram

The Hertzsprung-Russell diagram plots stellar temperature against luminosity, with the two sets of classes shown in Figure 1.3.

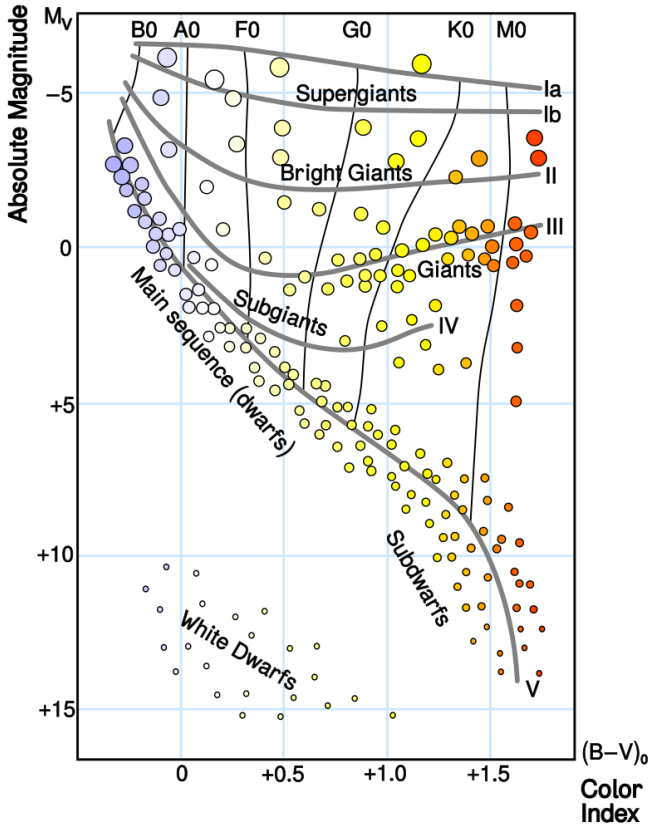

Figure 1.3: The Hertzsprung-Russell Diagram. Photometric colours can be used to gauge $T_{\rm EFF}$, while absolute magnitudes can be used to infer luminosities. As such, the "theoretical" HR diagram plotting luminosity against $T_{\rm EFF}$ is often shown in terms of observed quantities (i.e magnitudes vs colour). [Wikipedia]

1.4 M-dwarfs

Despite being the most common star in the universe, M-dwarfs are less-well understood than their more massive counterparts of other spectral types (Allard et al. 1992; Reid & Hawley 2005). Factors arising from their low masses, $T_{\rm EFF}$, and luminosities, plus the structure of their interior and atmosphere, must be taken into account when constructing theoretical models or studying them observationally:

- Dust formation (e.g. Tsuji et al. 1996a,b)
- Lack of continuum opacities due to extensive molecular absorption (e.g. Allard et al. 1992)
- Measuring continuum difficult due to extensive molecular absorption (e.g. TiO, VO, H_20, CO)
- Visible luminosity sensitive to metallicity (due to TiO and VO abundances, plus metallicity-$F_{\rm bol}$ relationship), not so for near-IR (and thus is a better metallicity probe) (Chabrier & Baraffe 2000; Delfosse et al. 2000)

- Convection (e.g. Hawley et al. 2000)
- Spectral type and colour relations (e.g. V-I & V-K) (Bessell 1991)

1.4.1 M-dwarf Stellar Models

Observations of M-dwarfs as a group have historically found radii to be larger (up to 10 %) and T_{Eff} cooler (up to 5 %) than predicted by theoretical models - a discrepancy that spanned nearly four decades (e.g. Hoxie 1973; Lacy 1977; Popper 1997; Clausen et al. 1999; Torres & Ribas 2002; Ribas 2003; López-Morales & Ribas 2005; Berger et al. 2006; Ribas 2006; López-Morales 2007; Ribas et al. 2008). More recent theoretical models narrow this discrepancy (e.g. Feiden & Chaboyer 2012, 2014; Torres et al. 2014), working towards a solution for radius inflation and temperature suppression in low-mass stars and into the regime where starspot uncertainties could account for the remaining discrepancy Feiden & Chaboyer (2012).

As to the cause of the problem, magnetic fields (due tidal interaction in tight binaries inhibiting convection) have been invoked as a physical explanation (e.g. Feiden & Chaboyer 2013a,b), as have the effects of missing opacity components/metallicity effects within the models themselves (e.g. Berger et al. 2006). Single stars targeted via interferometry are thus important to help constrain radii and T_{Eff} (being free of tidal effects) (e.g. Lane et al. 2001; Ségransan et al. 2003; Berger et al. 2006; Demory et al. 2009), as are wide binaries with long orbital periods (e.g. Doyle et al. 2011). Other systems also remain to be explained by models, such as an inflated single-star planet host, where the planet is on a wide enough orbit that tidal effects should be minimal (Charbonneau et al. 2009).

1.5 Exoplanet and Eclipsing Binary Detection

Known exoplanets now number in the thousands and have been found through utilisation of a variety of (often complementary) techniques. Such techniques are sensitive to different regions of the mass-separation parameter space, as demonstrated by Figure 1.4, where it is clear that the discoveries are dominated by planets found by the transit and RV methods. In general though, larger planets are easier to detect and most methods are more sensitive to planets with smaller separations (barring direct detection where larger separations are useful to separate the planet and star light contributions, and microlensing). Figure 1.4 shows a huge range in planetary characteristics, unfilled though the parameter space is.

1.5.1 Radial Velocity and the Keplerian Orbit

Just as stars influence the planets that orbit them, planets (or secondary stellar companions) influence their stellar hosts, with both bodies orbiting about a common centre of mass. Planets themselves are much too small and dim to directly observe RVs for, but can be indirectly observed via the slight motion they induce on their hosts. This movement is visible to an observer along the line of sight (thus giving no information for face-on systems) as small Doppler shifts in wavelength of the absorption lines composing the star's spectrum. From such instantaneous shifts, RVs can be derived, yielding information about both any bodies orbiting the star, but also the activity of the star itself. The technique requires a high degree of instrument stability, as well as wavelength calibration to minimise sources of instrumental drift such as thermal expansion/contraction of the spectrograph optics/mounts. Additional factors have to be taken into account, including the Earth/Sun motion, and stellar noise on the part of the observed star.

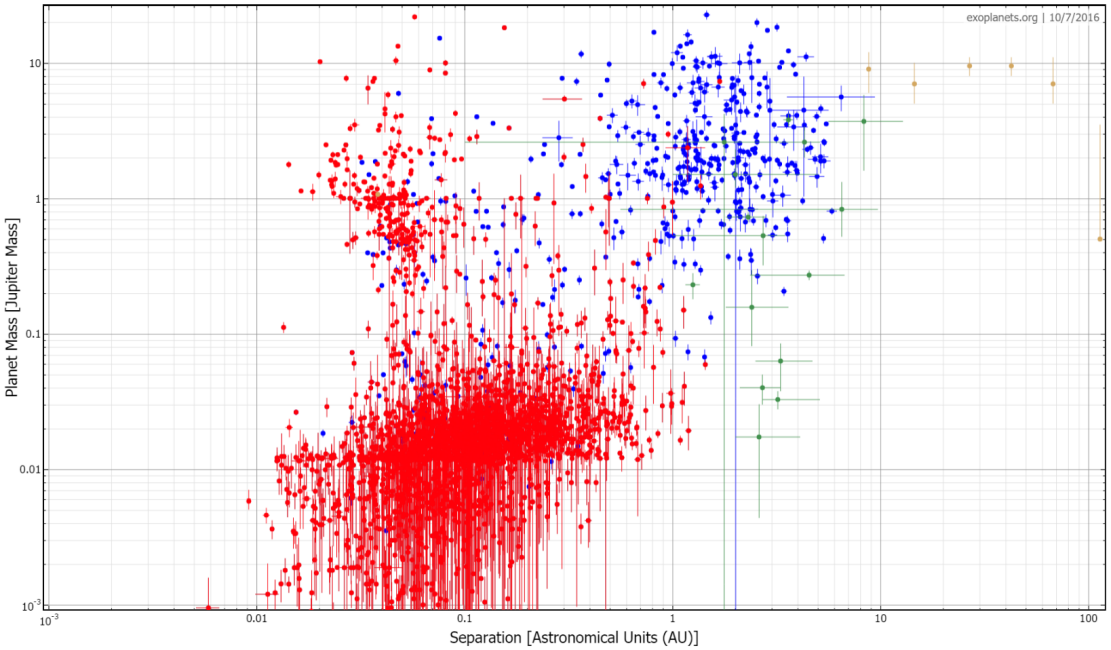

Figure 1.4: Planet mass (M_J) as a function of separation (AU) for all discovered planets as of October 2016. Points in red were found via transit, blue via radial velocity, green via microlensing and orange by direct detection [exoplanets.org]

A three dimensional Keplerian orbit is completely described by seven parameters:

1. a - semi-major axis of the elliptical orbit,
2. e - eccentricity of the elliptical orbit,
3. P - orbital period, related to a and the masses of the orbiting bodies through Kepler's 3rd law,
4. ν - position along orbital path (and thus related to the time of observations), also known as the true anomaly ,
5. i - orbital inclination ($0 \leq i < 180\,^\circ$, where $i = 0^\circ$ is a face on orbit),
6. Ω - longitude of the ascending node,
7. ω - argument of pericentre,

where a & e describe the shape of the orbit, i, Ω & ω describe the orientation of the orbital plane (relative to an observer), and ν describes the position of the orbiting body in its orbit. Figure 1.5 gives a visual representation of these parameters.

RV measurements are not able to grant insight into Ω and only reveal $a \sin i$, not a or i individually. The technique also only provides the *minimum* mass for an orbiting body (specifically the mass that can be inferred from the line-of-sight RV component), requiring knowledge of i to provide a more accurate mass. As such, another source of information is required to place limits on these parameters and fully define/constrain the orbit (Perryman 2011).

A more detailed overview of the radial velocity method can be found in Lovis & Fischer (2010).

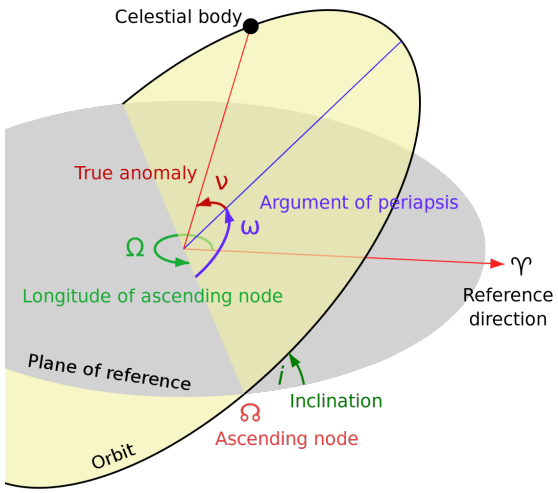

Figure 1.5: Diagram of an orbit and associated terms [Wikipedia]

1.5.2 Transits

For systems with favourable geometry, transits can be a very productive method of detecting and characterising planets or eclipsing binary star systems. At its most basic, detection of a body via the transit method involves observing a star for periodic decreases in total flux, associated with a body passing directly in front of its host star and blocking a fraction of its light, as per Figure 1.6. For larger/more reflective or self-luminous objects (i.e. stars, or in the IR for warm/hot planets), a second dip in flux is visible, known as the secondary eclipse, associated with the body passing *behind* its host star and no longer contributing its own light (reflected or otherwise). Transits provide insight into the orbital parameters of the system and relative dimensions of planet/secondary and host star. Additionally, eclipse timing gives insight into other massive bodies in the system, and transmission spectroscopy can be used to probe the atmosphere of a transiting planet.

In practice, many factors need to be taken into account to precisely constrain such properties including:

- Transit depth/shape
- System geometry (e.g. probability of eclipse, grazing eclipse, transit time)
- False positives
- Stellar factors/activity (e.g. limb darkening, spots)

Transit measurements alone do not provide the mass of the transiting body, but this can be obtained via follow-up RV measurements, with orbital inclination already well-constrained by the transiting system. For a thorough treatment of transits and occultations, see Winn (2010).

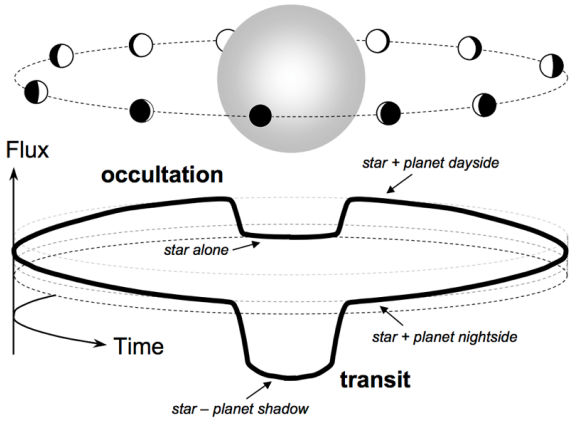

Figure 1.6: Illustration of geometry and flux levels, including the primary and secondary eclispses, over the complete orbital period of a transiting exoplanet Winn (2010)

1.6 The FunnelWeb Survey

The FunnelWeb Survey aims to conduct a complete (magnitude-limited) survey of the stars in the Southern Hemisphere. The details of the program are laid out in the following section, with more information available online at the survey website https://funnelweb.wikispaces.com/The+FunnelWeb+Survey.

1.6.1 Science Goals

Main survey goals:

- Spectral library including T_{Eff}, log(g), [Fe/H], and [alpha/Fe]
- Input catalogue for the Transiting Exoplanet Survey Satellite (TESS) (Ricker et al. 2015)
- Identification of young stars using Li (e.g. Soderblom 2010; Jeffries 2014)

1.6.2 The TAIPAN Instrument

TAIPAN (Kuehn et al. 2014; Content et al. 2016; Staszak et al. 2016) is a spectroscopic instrument located at the 1.2 m UK Schmidt Telescope at Siding Spring Observatory Australia. The instrument is fed by up to 300 independently-controlled robotic fibres, thus permitting massively parallel surveys (specifically the TAIPAN Galaxy Survey and the FunnelWeb Star Survey). Basic instrument parameters are as follows:

- 370-870 nm at R$\sim$2000
- 6° field of view
- 3.3 arcsec on-sky fibre diameter
- Field reconfiguration time $<$ 6 mins

1.6.3 Stellar Classification

FunnelWeb aims to employ a data-driven approach to stellar parameter determination (e.g. [Fe/H], T_{Eff}, log(g), spectral type), similar to that employed by The Cannon (Ness et al. 2015). The principle advantage of such a pipeline is its independence from models and spectral line lists, along with their associated uncertainties and limitations. Being data-driven, it is machine learning in nature, with the pipeline being trained upon a comprehensive set of standard stars with observationally well-constrained stellar parameters that span the multi-dimensional label-space. Accuracy is therefore dependent on having a wide-ranging and trustworthy set of such stars, free from any accuracy issues or simplifying assumptions involved in modelling (e.g. T_{Eff} determination via spectral methods being influenced by non-LTE or 3D effects (Yong et al. 2004; Bensby et al. 2014)) . As such, the standard stars should have their parameters determined by a method as model independent as possible.

1.6.4 Input Catalogue

FunnelWeb's input catalogue will be composed of the primary survey, Gaia G $<$ 12, DEC $\leq 0°$, $|b| \geq 10°$, and the following supplementary surveys:

- Galactic plane: Gaia G $<$ 12, DEC $\leq 0°$, -10° $\leq$ b $\leq$ 10°,
- Young stars,
- Metal poor stars,
- M-dwarfs and TESS targets (e.g. using Koen et al. 2002; Kilkenny et al. 2007; Lépine & Gaidos 2011),
- Northern Galactic archaeology,
- Infrared excess selected sample.

To enable FunnelWeb's data driven classification pipeline, it will observe a number of standard stars scattered across the stellar parameter space to serve as a training set. Such stars have been well-characterised in prior literature and possess precise values for some or all of the stellar labels used.

1.6.5 M-Dwarf Standards

Standard stars are of particular concern for M-dwarfs, whose parameters have historically been poorly estimated by stellar models (as detailed in 1.4.1). As compared to stars of other spectral types, there is a paucity of M-dwarfs with precise observationally measured radii, masses, and T_{Eff}, due in part to how faint such stars often are. Additionally, due to the complexity of their atmospheres, they often have poorly constrained metallicities and abundances.

As such, M-dwarf standards were selected from four main catagories of observations, each of which also ideally has a parallax measurement and constrains one or more stellar parameter:

1. M-dwarfs with measured interferometric diameters (e.g. Ségransan et al. 2003; Demory et al. 2009; Kervella et al. 2016),
2. M-dwarfs with metallicities measured from infrared spectra (e.g. Rojas-Ayala et al. 2012; Muirhead et al. 2012, 2014; Newton et al. 2014; Terrien et al. 2015)

3. M-dwarfs with an FGK common proper motion (CPM) companion (e.g. Mann et al. 2013; Newton et al. 2014),
4. M-dwarfs in double-lined eclipsing binaries (e.g. Kraus et al. 2011; Zhou et al. 2015; Lubin et al. 2017).

The majority of candidate stars fitting into these categories have DEC $\geq 0°$ and are thus generally unsuitable for FunnelWeb observation from Siding Spring. An incomplete selection of references to catalogues with M-dwarfs visible from the Southern Hemisphere has been provided above.

1.7 Follow-up Instruments & Ancillary Science Surveys

1.7.1 The HATSouth Exoplanet Survey

The HATSouth Exoplanet Survey (Bakos et al. 2013) is a network of automated telescopes across three sites, Siding Spring Observatory (Australia), Las Campanas Observatory (Chile), and HESS site (Namibia), capable of 24 hour observations of the entire Southern Hemisphere. High-precision light curves are obtained for fields monitored for extended periods of time, with the objective being the detection of exoplanetary transits. The program has a robust data management and candidate detection pipeline, with RV-follow up obtained for promising targets with increasingly higher-resolution spectrographs as non-planet detections are ruled out (e.g. eclipsing binaries, whose RV amplitudes are well above those of a transiting planet and can be ruled out early in bulk with lower-resolution instruments). As of July 2016, the program has discovered 35 exoplanets (de Val-Borro et al. 2016), along with several other notable eclipsing binary systems (Zhou et al. 2014, 2015).

1.7.2 Gaia

Gaia: (Gaia Collaboration et al. 2016b) is an ESA (European Space Agency) space telescope mission designed to undertake astrometric observations of the entire sky down to a Gaia G band magnitude of 20, compiling both the 3D spatial *and* velocity distributions of the stars within the Galaxy. The mission is the successor to ESA's previous astrometric mission, the HIPPARCOS satellite (ESA 1997), which measured parallaxes for approximately 118,000 objects. Gaia will observe 10^9 objects, all available to the public once processed, calibrated, and validated internally via regular data releases - the first of which was made available in November 2016 (Gaia Collaboration et al. 2016a; Lindegren et al. 2016).

1.7.3 TESS

TESS, the Transiting Exoplanet Survey Satellite (Ricker et al. 2015), is an upcoming NASA space mission designed primarily for exoplanet research. The mission aims to observe transits for at least 200,000 main sequence dwarfs each of which will be 10-100 time bright than those in the Kepler field, thus enabling ground based follow-up. TESS will observe 26 fields for durations varying from 27 days to 351 days, as shown in Figure 1.7, and is expected to find more than 1000 planets smaller than Neptune. The input catalogue for TESS has been compiled from existing surveys with the intent of observing the most promising targets, ruling out those unlikely to have short period planets (such as giants). The catalogue is somewhat dynamic, and will see modifications up to and beyond launch (Stassun et al. 2017).

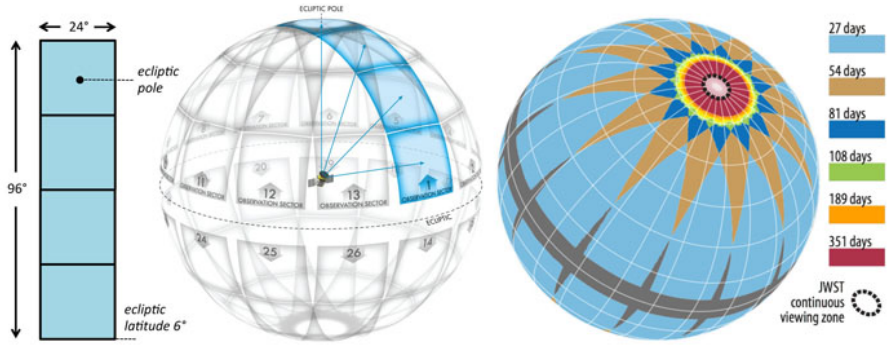

Figure 1.7: TESS fields of view. **Left:** Combined field of view enabled by TESS's four cameras. **Middle:** Observation fields on celestial sphere - 13 per hemisphere. **Right:** Duration of observations, taking into account overlap. [NASA]

1.7.4 Veloce

Veloce is a currently in-development ultra-stabilised high-resolution (R∼80,000) spectrograph in development for the AAT, due for comissioning in April 2018. When complete, the instrument will be capable of obtaining RVs at sub-m s^{-1} precision, giving it the ability to detect exoplanets about M-dwarfs and sun-like stars - a crucial ability in the post-TESS era. More information on Veloce can be found on the UNSW website as follows: https://newt.phys.unsw.edu.au/ cgt/Veloce/Veloce.html.

1.7.5 KELT

KELT, The Kilodegree Extremely Little Telescope, is a system of two photometric-survey telescopes located in the Northern (Pepper et al. 2007) and Southern (Pepper et al. 2012) Hemispheres (USA and South Africa respectively), providing a near-all-sky coverage. Like the HAT-South Exoplanet Survey, KELT observes exoplanetary transits about bright stars, in the process producing a number of non-planet candidates (e.g. eclipsing binaries) which do not form part of the core exoplanet search.

1.7.6 WiFES

WiFeS, the Wide Field Spectrograph (Dopita et al. 2007), is an instrument located at the ANU 2.3 m Telescope at Siding Spring Observatory. Providing remote operation, a wavelength range of 320-950 nm, high throughput (>30%), and spectral resolutions of R∼3,000 and R 7,000, the instrument is an ideal medium-resolution instrument for obtaining RV follow-up measurements.

1.7.7 LCOGT and NRES

LCOGT, The Las Cumbres Observatory Global Telescope Network (Pickles et al. 2014) , is a global network of robotic telescopes for photometric and spectroscopic follow-up observations. Composed of a mix of 2 , 1 , and 0.4 m telescopes, the network covers a range of latitudes and longitudes allowing for continuous, all-sky observations. NRES, the Network of Robotic Echelle

Spectrographs (Siverd et al. 2016), will be six identical, fibre-fed, optical echelle spectrographs (R∼53,000, 390-860 nm) deployed across the LCOGT network. Being robotic, the network schedules observations and automates data reduction, making it well suited to capturing stellar or exoplanet transits, or getting good RV phase coverage for orbits. Further information can be located on the observatory's website https://lco.global/astronomers/.

1.7.8 VLTI & PIONIER

PIONIER, the Precision Integrated-Optics Near-Infrared Imaging ExpeRiment (Bouquin et al. 2011), is an interferometric instrument on the VLTI (Very Large Telescope Interferometer) at Paranal Observatory. It is capable of combining the beams from the four 8 m telescopes, or the four 1.8 m auxiliary telescopes, to form a high-angular resolution instrument.

Chapter 2

Proposal

2.1 Supervisory Panel

Table 2.1 shows the supervisory panel, along with key expertise of each member.

Table 2.1: Supervisory panel

Name	Role	Expertise
A/Prof. Michael Ireland	Primary Supervisor	Young stars/planets, optical interferometry, pipelines
Prof. Michael Bessell	Supervisory Panel	Spectro/photometry, metal-poor objects
Dr. Luca Casagrande	Supervisory Panel	Photometry, photometric T_{Eff} determination
Dr. Marusa Zerjal	Supervisory Panel	Young/active stars, data-driven approaches

2.2 Precision Angular Diameters of Southern Hemisphere Spectral Type Standards

Aim: Obtain high precision ($\leq$1%) interferometric diameters for Southern Hemisphere spectral type standards to anchor the T_{Eff} for large, high-SNR stellar surveys (i.e. FunnelWeb).

Motivation: Interferometry is one of the few methods of observationally determining stellar diameters, and thus T_{Eff}. Such measurements provide crucial tests for models, anchor empirical relations, and importantly can serve as spectral standards for large stellar surveys (including Gaia and FunnelWeb). Existing work has not spanned stellar evolutionary state (e.g. just dwarfs, or just giants, not sub-giants), and has had poor connection to spectroscopic metallicities. Thus this project has selected a set of dwarfs and sub-giants for observation.

Methodology: Use the shortest-wavelength, highest-precision beam combiner at VLTI (PIONIER) on the longest baselines to observe a selection of Southern Hemisphere spectral standards to obtain precise angular diameters. Use these diameters to derive precision T_{Eff}, as well as resolving metallicity and gravity effects.

Facilities: VLTI & PIONIER

Dataset: VLTI & PIONIER data, Gaia DR1 & DR2

Collaborators: FunnelWeb personnel, Dr. Tim White (Aarhus University), Dr. Iva Karovicova (Heidelberg University), Assistant Professor Fabien Baron (Georgia State University), Professor Jean Baptiste Bouquin (IPAG)

Risks: Poor weather/technical difficulties when observing

Papers: Precision Angular Diameters of Southern Hemisphere Spectral Type Standards (Lead author), Metallicity and Gravity Corrections to the Colour-Effective Temperature Scale Across the HR-Diagram (Lead or co-author)

2.3 A Data Driven Stellar Classification Pipeline for the FunnelWeb Star Survey

Aim: Development of a data-driven (i.e. model free) stellar classification pipeline for FunnelWeb able to type and produce stellar parameters for M-dwarfs

Motivation: M-dwarf parameters are often poorly reproduced by theoretical stellar models, which gives rise to uncertainties when compared to observational data for classification purposes. A *data-driven* method is free of this issue, instead deriving its accuracy from a training set of observationally well-constrained objects spanning parameter space. Such an approach is a model and spectral line list independent method of stellar parameter determination for such parameters as metallicity ([Ti/H] and [O/H] for M-dwarfs), T_{Eff}, log(g), and spectral type. Similar methods exist, such as The Cannon (Ness et al. 2015), but currently do not perform well across the entire HR diagram.

Methodology: Standard stars with uncertainties at the few percent level will be selected from the literature prior to work beginning on the pipeline to ensure that they are on the target list for FunnelWeb and obtain high SNR spectra. Such stars will be drawn from three main categories, with a fourth possible depending on pipeline specifics:

1. M-dwarfs with measured interferometric diameters,
2. M-dwarfs with metallicities measured from infrared spectra
3. M-dwarfs with an FGK common proper motion (CPM) companion,
4. M-dwarfs in double-lined eclipsing binaries.

The pipeline will be developed collaboratively within the FunnelWeb team by those with similar research interests as the end result will serve the entire collaboration. Development will be undertaken in Python, the current standard language of the astronomy community and one that is in demand outside as to ensure the development of transferable skills. Preliminary prototyping has been undertaken by M. Ireland using a grid of model spectra and the Local Tangent Space Alignment (LTSA) algorithm as per Yang et al. (2006). LTSA presents advantages to The Cannon in that it is highly-non-linear, as contrasted with quadratic approach of The Cannon, allowing it to better capture the different physics occurring at differing spectral types (thus having better

potential to work across the HR diagram). Once complete, the pipeline will be trained upon the standard stars, before producing stellar parameters for all input stars.

The Cannon itself remains a valid alternative method for deriving parameters of *well-defined* regions of the parameter space. As such, an investigation will be conducted into whether it alone is sufficient for classifying M-dwarfs via a quadratic approach, and how it compares to the developed non-linear LTSA pipeline.

Facilities: TAIPAN & UK-Schmidt Telescope

Dataset: Model spectra for prototyping, FunnelWeb spectra, literature results for standard stars

Analysis: The measure of success for the pipeline will be both how well it reproduces the stellar parameters of the training set when employing a cross-validation approach - that is training on only a subset of the standard stars and accurately reproducing parameters for unseen (but well-characterised) objects.

Collaborators: FunnelWeb personnel

Risks: Insufficient stellar standards to span label space

Paper: The FunnelWeb Survey: M-dwarf Stellar Parameters Using Sparse Labels and a Data-driven Pipeline (Lead author)

2.4 A Catalogue of Southern Hemisphere M-dwarfs with the FunnelWeb Star Survey

Aim: Produce a complete (but magnitude limited) M-dwarf catalogue of the Southern Hemisphere stars observed by the FunnelWeb Star Survey, with stellar parameters obtained from FunnelWeb's data-driven classification pipeline

Motivation: Enabled by FunnelWeb's data-driven classification pipeline, it will be possible to produce catalogues of stars and their parameters for different Southern Hemisphere stellar populations. One such population are M-dwarfs, interesting because they comprise part of the low mass region of the main sequence, possessing complex atmospheric chemistry and being correspondingly difficult to model accurately. M-dwarfs are also of interest in the exoplanet era, due to potentially Earth-like planets being easier to detect around them given their lower masses and luminosities (by way of the planetary "habitable" zone being closer to the star where transit and RV detection methods are more sensitive). As such, a complete (but magnitude limited) M-dwarf catalogue of the southern sky, along with derived stellar parameters, would be a useful result from the FunnelWeb Star Survey, and provide great utility to the field (particularly when combined with Gaia DR2 parallaxes). Such a catalogue could, if compiled by early-mid 2018 to meet launch, serve as an input catalogue to the TESS mission (the TESS input catalogue (Stassun et al. 2017) remains somewhat dynamic and will see additions and improvements up-to and beyond launch). Failing that, the catalogue would still prove crucially useful in providing stellar parameters for all M-dwarfs observed by TESS, better enabling the study and

characterisation of any exoplanets found about such stars.

Methodology: Compile stars observed with FunnelWeb (vetting for non-single stars or other anomalous systems that might classify poorly), classify using FunnelWeb's data-driven classification pipeline, further vet results for anomalies, collate (possibly combine with Gaia DR2 information), and publish

Facilities: TAIPAN & UK-Schmidt Telescope

Dataset: FunnelWeb spectra, Gaia DR1 & DR2

Collaborators: FunnelWeb personnel

Risks: Issues with FunnelWeb classification pipeline (i.e insufficient M-dwarf standards)

Paper 1: The FunnelWeb Survey: A Catalogue of Southern Hemisphere M-dwarfs (Lead author)

2.5 Constraining the T_{Eff} Scale of M-dwarfs with HATSouth, FunnelWeb and Gaia

Aim: Locate and characterise yet-unstudied low-mass double-lined eclipsing binaries observed (but not followed-up) by the HATSouth Exoplanet Survey to place observational constraints on M-dwarfs, the planets that orbit them, their stellar models, and empirical relations.

Motivation: Due to their intrinsic faintness, few M-dwarfs have accurate observationally derived masses, diameters, and effective temperatures. Such stellar parameters have historically been poorly predicted by models by as much as 5-10%, partly due to the paucity of observationally constrained stars to anchor them. This project would set out to increase the number of known M-dwarfs with accurately measured masses, radii, and T_{Eff}, addressing both the low numbers of well-studied low-mass double-lined eclipsing binaries in general, but also the dearth of such stars in the southern sky. Addressing both of these points aids not just the field as a whole in terms of testing models and calibrating empirical relations, but more specifically the accuracy of FunnelWeb's data-driven stellar classification pipeline by having more standards available for observation in the southern hemisphere.

Methodology: Locate yet-uncharacterised candidate low-mass double-lined eclipsing binaries from HATSouth light-curves, obtain FunnelWeb spectra to perform preliminary characterisation and vetting (by way of RVs and spectral typing), before conducting more detailed follow up (including use of Gaia DR2, high-precision photometry, and high-resolution spectroscopy).

Facilities: TAIPAN & UK-Schmidt Telescope, ANU 2.3 m Telescope & WiFeS, LCOGT & NRES

Dataset: Pre-existing HATSouth Exoplanet Survey light-curves, FunnelWeb spectra, spectroscopic and photometric follow-up observations, Gaia DR1 & DR2

Analysis: Accurate observationally derived stellar parameters for an eclipsing binary rely on knowledge of the Keplerian orbit by way of RVs (for stellar masses), stellar transits (for relative stellar radii), and parallax (to enable the relative radii to be put on an absolute scale, and to be converted to an angular diameter for T_{Eff} computation). HATSouth light curves will provide accurate orbital periods (as a result of the higher number of transits observed) and preliminary primary and secondary eclipse (i.e. transit) measurements, to be better constrained with higher-precision photometric follow-up observations by the automated LCOGT network. Such follow-up observations will ideally be multi-wavelength to assist in breaking the limb-darkening orbital eccentricity degeneracy. Necessary corrections will be made for the effects of limb-darkening and partial (i.e. grazing) transits, with additional allowances made for stellar activity (i.e. spots).

The Keplerian orbit will be determined by a combination of FunnelWeb RVs, and follow-up medium-to-high-resolution spectroscopic measurements over the orbit duration (a period of a few days for most eclipsing binaries) with WiFES on the ANU 2.3 m Telescope, and NRES on LCOGT. Comparison to the photometric observations will allow the orbital inclination, degenerate for RV measurements alone, to be constrained. For fainter stars without pre-existing measurements from TGAS, parallaxes will be obtained from Gaia DR2 (expected release: April 2018).

Additionally, spectroscopic follow-up will enable spectral analysis of each component of the binary - both for the purpose of preliminary vetting via typing, and abundance/metallicity determination. Low-to-medium-resolution spectra presents the widest spectral coverage and highest SNR, but will be insufficient to resolve each of the binary components, necessitating the treatment of them as a single star for the analysis. High-resolution spectra, provided the object in question is bright enough to allow for sufficient SNR, will be capable of this separation.

Collaborators: FunnelWeb personnel, Assistant Professor Gaspar Bakos (Princeton University, HATSouth Exoplanet Survey) & Dr. George Zhou (Harvard-Smithsonian Center for Astrophysics, HATSouth Exoplanet Survey)

Risks: Yield unclear, potential difficulties in collaborating with HATSouth team - will need to be explored prior to committing major time/resources

Paper: The FunnelWeb Survey: A New Set of Southern Hemisphere M-dwarf Eclipsing Binaries with FunnelWeb, HATSouth, and Gaia (Lead author)

2.6 Related Projects

Follow-up observations of M-dwarf catalogue with Veloce.

Follow-up RV observations of HATSouth and TESS targets with FunnelWeb RVs.

Expanding project eclipsing binary project to include KELT data.

2.7 Timeline

Table 2.2: Proposed PhD timeline

Timeline	Item
2017	
30/01/2017	PhD Start
23/06/2017	PhD proposal due
29-30/06/2017	PhD proposal talk
06-08/07/2017	Harley Wood Winter School for Astronomy
09-14/07/2017	ASA Annual Scientific Meeting
–/07-09/2017	VLTI Period 99B (PIONIER Observations)
–/09/2017	FunnelWeb Survey begins
–/11/2017	7th Australian Exoplanet Workshop
–/12/2017	Mount Stromlo Student Seminars
–/12/2017	Interferometric diameters paper
2018	
–/01/2018	Veloce commissioning at AAT
–/04/2018	Gaia DR2
–/06/2018	Annual review talk/report
–/07/2018	ASA Annual Scientific Meeting
–/07/2018	TESS Launch, beginning of observations in southern hemisphere
–/11/2018	8th Australian Exoplanet Workshop
–/12/2018	Mount Stromlo Student Seminars
–/12/2018	FunnelWeb pipeline paper
2019	
–/06/2019	Annual review talk/report
–/07/2019	ASA Annual Scientific Meeting
–/11/2019	9th Australian Exoplanet Workshop
–/12/2019	Mount Stromlo Student Seminars
–/–/2019	M-dwarf catalogue paper
–/–/2019	Eclipsing binary paper
–/–/2019	TESS observations of northern hemisphere begin (+South DR)
2020	
30/01/2020	3 year mark
–/–/2020	Submission
–/–/2020	Final thesis seminar
30/07/2020	3.5 year mark

Bibliography

Allard, F., Scholz, M., & Wehrse, R. 1992, Revista Mexicana de Astronomia y Astrofisica, vol. 23, 23, 203

Bakos, G. Á., Csubry, Z., Penev, K., et al. 2013, Publications of the Astronomical Society of the Pacific, 125, 154

Bensby, T., Feltzing, S., & Oey, M. S. 2014, Astronomy and Astrophysics, 562, A71

Berger, D. H., Gies, D. R., McAlister, H. A., et al. 2006, The Astrophysical Journal, 644, 475

Bessell, M. S. 1991, The Astronomical Journal, 101, 662

Bouquin, J.-B. L., Berger, J.-P., Lazareff, B., et al. 2011, Astronomy & Astrophysics, 535, A67

Buchhave, L. A. & Latham, D. W. 2015, The Astrophysical Journal, 808, 187

Chabrier, G. & Baraffe, I. 2000, Annual Review of Astronomy and Astrophysics, 38, 337

Charbonneau, D., Berta, Z. K., Irwin, J., et al. 2009, Nature, 462, 891

Clausen, J. V., Baraffe, I., Claret, A., & Vandenberg, D. A. 1999, in , 265

Content, R., Lawrence, J., Gers, L., & Zhelem, R. 2016, in , 990888

de Val-Borro, M., Bakos, G. Á., Brahm, R., et al. 2016, The Astronomical Journal, 152, 161

Delfosse, X., Forveille, T., Ségransan, D., et al. 2000, Astronomy and Astrophysics, 364, 217

Demory, B.-O., Ségransan, D., Forveille, T., et al. 2009, Astronomy and Astrophysics, 505, 205

Dopita, M., Hart, J., McGregor, P., et al. 2007, Astrophysics and Space Science, 310, 255

Doyle, L. R., Carter, J. A., Fabrycky, D. C., et al. 2011, Science, 333, 1602

ESA. 1997, in

Feiden, G. A. & Chaboyer, B. 2012, The Astrophysical Journal, 757, 42

Feiden, G. A. & Chaboyer, B. 2013a, Proceedings of the International Astronomical Union, 9, 150

Feiden, G. A. & Chaboyer, B. 2013b, The Astrophysical Journal, 779, 183

Feiden, G. A. & Chaboyer, B. 2014, Astronomy and Astrophysics, 571, A70

Fischer, D. A. & Valenti, J. 2005, The Astrophysical Journal, 622, 1102

Fitzgerald, M. P. 1970, Astronomy and Astrophysics, 4, 234

Gaia Collaboration, Brown, A. G. A., Vallenari, A., et al. 2016a, Astronomy and Astrophysics, 595, A2

Gaia Collaboration, Prusti, T., de Bruijne, J. H. J., et al. 2016b, Astronomy and Astrophysics, 595, A1

Gillon, M., Triaud, A. H. M. J., Demory, B.-O., et al. 2017, Nature, 542, 456

Gonzalez, G. 1997, Monthly Notices of the Royal Astronomical Society, 285, 403

Gray, D. F. 2008, The Observation and Analysis of Stellar Photospheres, 3rd edn. (Cambridge University Press)

Habets, G. M. H. J. & Heintze, J. R. W. 1981, Astronomy and Astrophysics Supplement Series, 46, 193

Hawley, S., Reid, I. N., & Gizis, J. 2000, in From Giant Planets to Cool Stars, Vol. 212, 252

Hoxie, D. T. 1973, Astronomy and Astrophysics, 26, 437

Jeffries, R. D. 2014, in , eprint: arXiv:1404.7156, 289–325

Johnson, H. L. 1965, The Astrophysical Journal, 141, 923

Kervella, P., Mérand, A., Ledoux, C., Demory, B.-O., & Le Bouquin, J.-B. 2016, Astronomy and Astrophysics, 593, A127

Kilkenny, D., Koen, C., van Wyk, F., Marang, F., & Cooper, D. 2007, Monthly Notices of the Royal Astronomical Society, 380, 1261

Koen, C., Kilkenny, D., van Wyk, F., Cooper, D., & Marang, F. 2002, Monthly Notices of the Royal Astronomical Society, 334, 20

Kraus, A. L., Tucker, R. A., Thompson, M. I., Craine, E. R., & Hillenbrand, L. A. 2011, The Astrophysical Journal, 728, 48

Kuehn, K., Lawrence, J., Brown, D. M., et al. 2014, in SPIE 9147, Vol. 9147, 914710

Lacy, C. H. 1977, The Astrophysical Journal Supplement Series, 34, 479

Lane, B. F., Boden, A. F., & Kulkarni, S. R. 2001, The Astrophysical Journal Letters, 551, L81

Lépine, S. & Gaidos, E. 2011, The Astronomical Journal, 142, 138

Lindegren, L., Lammers, U., Bastian, U., et al. 2016, Astronomy and Astrophysics, 595, A4

López-Morales, M. 2007, The Astrophysical Journal, 660, 732

López-Morales, M. & Ribas, I. 2005, The Astrophysical Journal, 631, 1120

Lovis, C. & Fischer, D. 2010, in Exoplanets, 27–53

Lubin, J. B., Rodriguez, J. E., Zhou, G., et al. 2017, ArXiv e-prints, 1706, arXiv:1706.02401

Mamajek, E. E., Torres, G., Prsa, A., et al. 2015, arXiv:1510.06262 [astro-ph], arXiv: 1510.06262

Mann, A. W., Brewer, J. M., Gaidos, E., Lépine, S., & Hilton, E. J. 2013, The Astronomical Journal, 145, 52

Mann, A. W., Gaidos, E., Lépine, S., & Hilton, E. J. 2012, The Astrophysical Journal, 753, 90

Muirhead, P. S., Becker, J., Feiden, G. A., et al. 2014, The Astrophysical Journal Supplement Series, 213, 5

Muirhead, P. S., Hamren, K., Schlawin, E., et al. 2012, The Astrophysical Journal Letters, 750, L37

Ness, M., Hogg, D. W., Rix, H.-W., Ho, A. Y. Q., & Zasowski, G. 2015, The Astrophysical Journal, 808, 16

Neves, V., Bonfils, X., Santos, N. C., et al. 2012, Astronomy and Astrophysics, 538, A25

Neves, V., Bonfils, X., Santos, N. C., et al. 2013, Astronomy and Astrophysics, 551, A36

Newton, E. R., Charbonneau, D., Irwin, J., et al. 2014, The Astronomical Journal, 147, 20

Pepper, J., Kuhn, R. B., Siverd, R., James, D., & Stassun, K. 2012, Publications of the Astronomical Society of the Pacific, 124, 230

Pepper, J., Pogge, R. W., DePoy, D. L., et al. 2007, Publications of the Astronomical Society of the Pacific, 119, 923

Perryman, M. 2011, The Exoplanet Handbook (Cambridge University Press)

Pickles, A., Hjelstrom, A., Boroson, T., et al. 2014, in , eprint: arXiv:1407.3284, 914912

Popper, D. M. 1997, The Astronomical Journal, 114, 1195

Reid, I. N. & Hawley, S. L. 2005, New light on dark stars : red dwarfs, low-mass stars, brown dwarfs, dOI: 10.1007/3-540-27610-6

Ribas, I. 2003, Astronomy and Astrophysics, 398, 239

Ribas, I. 2006, Astrophysics and Space Science, 304, 89

Ribas, I., Morales, J. C., Jordi, C., et al. 2008, Memorie della Societa Astronomica Italiana, 79, 562

Ricker, G. R., Winn, J. N., Vanderspek, R., et al. 2015, Journal of Astronomical Telescopes, Instruments, and Systems, 1, 014003

Rojas-Ayala, B., Covey, K. R., Muirhead, P. S., & Lloyd, J. P. 2012, The Astrophysical Journal, 748, 93

Ségransan, D., Kervella, P., Forveille, T., & Queloz, D. 2003, Astronomy and Astrophysics, 397, L5

Siverd, R. J., Brown, T. M., Hygelund, J., et al. 2016, in , 99086X

Soderblom, D. R. 2010, Annual Review of Astronomy and Astrophysics, 48, 581

Sousa, S. G., Santos, N. C., Mayor, M., et al. 2008, Astronomy and Astrophysics, 487, 373

Stassun, K. G., Oelkers, R. J., Pepper, J., et al. 2017, ArXiv e-prints, 1706, arXiv:1706.00495

Staszak, N. F., Lawrence, J., Zhelem, R., et al. 2016, in , 991223

Terrien, R. C., Mahadevan, S., Deshpande, R., & Bender, C. F. 2015, The Astrophysical Journal Supplement Series, 220, 16

Torres, G. & Ribas, I. 2002, The Astrophysical Journal, 567, 1140

Torres, G., Sandberg Lacy, C. H., Pavlovski, K., et al. 2014, The Astrophysical Journal, 797, 31

Tsuji, T., Ohnaka, K., & Aoki, W. 1996a, Astronomy and Astrophysics, 305, L1

Tsuji, T., Ohnaka, K., Aoki, W., & Nakajima, T. 1996b, Astronomy and Astrophysics, 308, L29

Wang, J. & Fischer, D. A. 2015, The Astronomical Journal, 149, 14

Winn, J. N. 2010, arXiv:1001.2010 [astro-ph], arXiv: 1001.2010

Yang, X., Fu, H., Zha, H., & Barlow, J. 2006, in Proceedings of the 23rd International Conference on Machine Learning, ICML '06 (New York, NY, USA: ACM), 1065–1072

Yong, D., Lambert, D. L., Prieto, C. A., & Paulson, D. B. 2004, The Astrophysical Journal, 603, 697

Zhou, G., Bayliss, D., Hartman, J. D., et al. 2014, Monthly Notices of the Royal Astronomical Society, 437, 2831

Zhou, G., Bayliss, D., Hartman, J. D., et al. 2015, Monthly Notices of the Royal Astronomical Society, 451, 2263